JOURNAL OF MATERIALS SCIENCE 29 (1994) 5947–5952

Strength estimation for silicon nitride specimens with a spherical void

M. KAJI, S. YOSHIURA, M. NISHIMURA
Central Research Laboratory, Kyocera Corporation, 1-4 Yamashita-cho, Kokubu, Kagoshima 899-43, Japan

Silicon nitride specimens embedded with a single spherical void were prepared for a flexural strength test. The measured flexural strengths of the specimens were compared with theoretically estimated strengths. Estimation of the strengths was done using a Gibbs free-energy criterion. The energy was calculated by Eshelby's equivalent inclusion method for a specimen with an embedded void. Good correspondence was obtained between the experimental and the estimated fracture loads. A deviation of the estimated strength from the experimental value was observed for voids whose diameters were comparable with intrinsic defects.

1. Introduction

Fracture origins in ceramics are usually either intrinsic defects or machined flaws. The strength of ceramics is often determined by intrinsic defects such as inclusions, voids or elongated grains [1], and it has been interesting to study the mechanisms of fracture which occurs from these defects. The fracture of brittle materials has generally been discussed in terms of the propagation of a crack already existing in the materials.

Several studies have been performed to evaluate the strength of silicon nitride containing artificial voids. Munz *et al.* [2] reported that a peripheral crack model can predict that the strength decreases with increasing flaw size for both reaction-bonded and sintered silicon nitride, if an appropriate length of annular crack is chosen. Okada and Hirosaki [3] also discussed circumferential cracking with artificially introduced voids and Heinrich and Munz [4] studied the strength of silicon nitride specimens with artificially introduced spherical surface pores. The same authors [5] also reported that the circumferential crack extension of the hemispherical pits should have occurred during loading from one grain diameter to approximately ten grain diameters, if an explanation based on fracture mechanics is possible. Analyses of the stress intensity factors have also been performed for a peripheral crack around the equator of spherical voids [6–12], and hemispherical pits [6, 7].

Here, fracture has been investigated from a different view point which does not need a circumferential crack. We consider that fracture occurs when a material becomes energetically unstable. To simplify the problem, a ceramic specimen which contains one artificial void was studied for a fracture condition of brittle materials. In the present study, the flexural strength of silicon nitride was considered.

The effect of fracture conditions is discussed on the unstable energy criterion, and procedures for calculation of the energy and an estimation of the strength are explained, as is the experimental procedure of the flexural test and the results. The fracture loads were calculated and compared with the experimental results. In the Appendix, the disturbed strain energy caused by a void is formulated micromechanically, using Eshelby's equivalent inclusion method [13].

2. Strength estimation procedure

2.1. Consideration of fracture conditions

The purpose of the present work is to estimate the strength by an energy criterion. We consider that fracture of ceramics occurs when a specimen containing a void becomes energetically unstable. When this unstable condition is satisfied, fracture occurs and cracks may initiate somewhere around a void and propagate in some direction. The shapes of the cracks and the propagation directions are dependent on the microstructures of the material and the applied stress states around the void. How these cracks are generated or propagated is not discussed here. We consider that crack initiation itself is the fracture.

This criterion is somewhat different from Griffith's energy theory of fracture mechanics. Griffith's theory states that a crack growth can occur if the energy required to form an additional crack size can just be delivered by the system under a constant load [14]. The difference between the previous works [2–5] on the fracture mechanics and the present work is that the former are based on a crack's existence and its propagation. The latter deals with the unstable energy condition for crack initiation.

2.2. Definition of fracture load

The Gibbs free energy describes an energy state of matter which is subjected to an external force. Under constant load, the relationship between the Gibbs free energy of a specimen and the void diameter is as

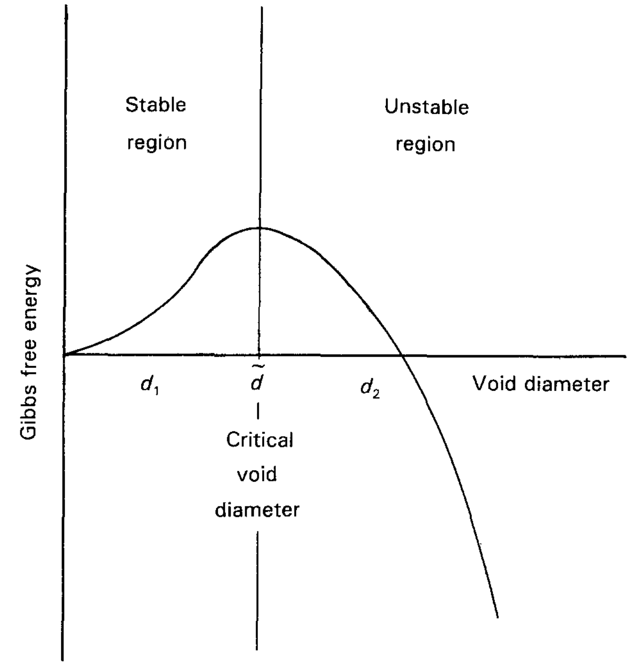

Figure 1 Relationship between void diameter and Gibbs free energy.

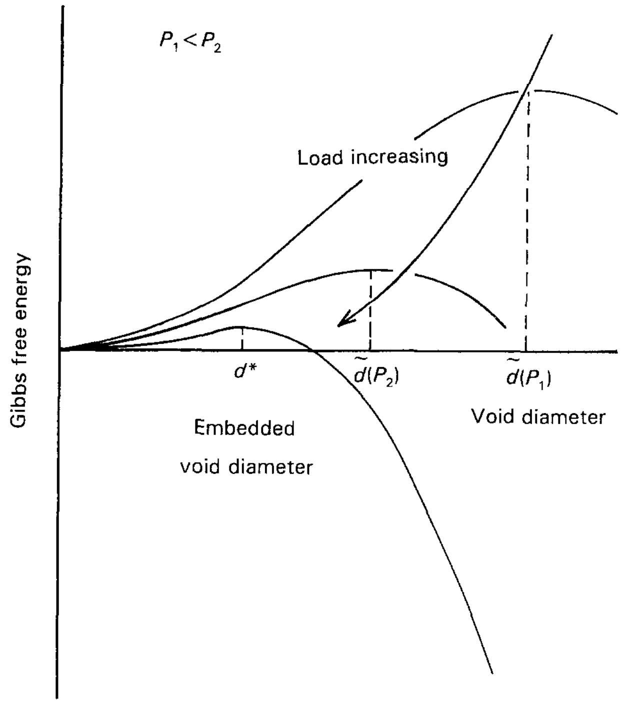

Figure 2 Fracture-load definition.

shown schematically in Fig. 1. The energy has a maximum at some void diameter; a critical void diameter $\tilde{d}$. The specimen is considered to be unstable beyond that point, because the energy is lower for a larger void diameter. A specimen with a void of diameter, d_1 is stable, but one with a void of diameter, d_2, is unstable.

As shown in Fig. 2, when the applied load, P, is increased from P_1 to P_2, the critical diameter is shifted to a smaller value. Eventually, the diameter becomes equal to the diameter of an embedded void, d^*. The corresponding load is defined as the fracture load.

2.3. Gibbs free energy

The Gibbs free energy of a specimen containing a void can be expressed by [15]

$$F = F^{S} + F^{E} + F^{I} \tag{1}$$

where F^{S} is the total surface energy of a specimen and presented as

$$F^{S} = F^{SV} + F^{SS} = \gamma S + \gamma^* S^* \tag{2}$$

where F^{SV} and F^{SS} are surface energies of a void and the specimen, respectively. γ and γ^* are the surface energies per unit area for the void and the specimen, respectively. S and S^* are surface areas of the void and the specimen, respectively.

F^{E} is the elastic strain energy of a specimen with no void, subjected to an external force. This is written as

$$F^{E} = \frac{1}{2}\int_{D} \sigma_{ij}^{A} u_{i,j}^{A}\, dx - \int_{|D|} X_i u_i^{A}\, dS \tag{3}$$

where σ_{ij}^{A}, $u_{i,j}^{A}$ and u_i^{A} are the stress, the total strain and the displacement, respectively, caused by the external force. X_i is the surface traction (external force). D represents the domain of the specimen with no void. $|D|$ means the surface of D.

F^{I} is the elastic stain energy of the specimen by the interaction between a void and an external force

$$F^{I} = -\frac{1}{2}\int_{\Omega} \sigma_{kl}^{A} e_{kl}^{*} dx \tag{4}$$

where Ω represents the domain of the void and e_{kl}^{*} is an eigenstrain due to the void [16]. This energy comes from the local strain field, disturbed around the void.

2.4. Fracture-load estimations

Let us consider two specimens; a specimen with a given void and another specimen with a void whose diameter is slightly larger than the given diameter. When the Gibbs free energy of the latter specimen is smaller than that of the former specimen, the specimen of the given diameter is in the unstable region. Therefore, to estimate the fracture load, only the difference of the Gibbs free energies for different void diameters is required. The difference of the free energies is determined by only the surface energy of the void, F^{SV}, and the interaction energy, F^{I}, because other terms are independent of the void diameter. Namely, the fracture condition is determined by the balance between the surface energy of the void and the interaction energy of a specimen.

The surface energy, contributing to the difference of the free energy, is the first term of Equation 2. The fracture surface energy per unit area, γ, is obtained using the equation [17]

$$\gamma = K_{IC}^2(1 - \nu^2)/2E \tag{5}$$

where K_{IC} is the fracture toughness. The K_{IC} of silicon nitride is 6.0 MPam$^{1/2}$ as is obtained by the single-edge precracked-beam (SEPB) method [18]. E is the Young's modulus and ν is Poisson's ratio.

The elastic strain energy from the interaction between the external force and a void, F^1 (Equation 4), is micromechanically calculated, using Eshelby's equivalent inclusion model. The derivations are shown in the Appendix. The calculation was performed on the basis of the following three assumptions. (1) The silicon nitride matrix is an isotropic and homogeneous material, because the grain size is small enough. (2) The void is not so close to the surface of a specimen that the disturbed strain is not affected by the surface. (3) There is no interaction between the artificially embedded void and intrinsic flaws.

In the practical calculation of the fracture load, we compared the Gibbs free energies of two specimens whose void diameters are $a_1 = a_2 = a_3 = a$ and $a_1 = a_2 = a_3 = 1.01a$. The comparison starts at a certain given load. The calculation is carried out step-by-step by increasing the load until the Gibbs free energy of the latter specimen becomes less than that of the former specimen. The load which satisfies the condition is the fracture load of a specimen. Estimations were also made with other conditions, such as a spherical enlargement of 1.02 or ellipsoidal enlargement. In either way, we obtained essentially the same results.

3. Experimental procedure

Mechanical properties of sintered silicon nitride are listed in Table 1. The material was prepared in the following manner. The silicon nitride powders were granulated and pressed in a die with a single spherical organic particle. The particle was put into a central area close to the tensile surface of the specimen. We used four grades of particle diameter, with fifty specimens being made for each grade.

The four-point bend test was carried out by JIS R 1601. The cross-section of the specimen was 3 mm in height and 4 mm in width. The inner and outer spans were 10 and 30 mm, respectively. The crosshead speed was 0.5 mm min^{-1}.

Specimens fractured from the introduced void were used to determine strength. The diameter of the void and the depth from the tensile surface were measured from scanning electron micrographs.

4. Results

The results are summarized in Table II. Average diameters of the four grades of voids were 153, 241, 312 and 470 μm, respectively. Several specimens of the 153 μm voids fractured from origins other than the artificially introduced voids. Several specimens of the 470 μm voids were discarded, because those voids appeared on the surface after machining. Scanning electron micrographs of typical voids are shown in Fig. 3. The voids possess good spherical shape.

The strength of the specimen varies because the diameter and the depth of voids are scattered. The nominal flexural strength is plotted as a function of the void diameter in Fig. 4. As the void diameter increases, the flexural strength decreases. The nominal flexural strength is also plotted as a function of void depth (the distance from the void surface to the specimen tensile surface) in Fig. 5. As the void depth decreases, the flexural strength decreases. This behaviour was qualitatively expected.

TABLE I Mechanical properties of silicon nitride

Bulk density	3.2 g/cm^{-3}
Vicker's hardness	14.4 GPa
Young's modulus	294 GPa
Poisson's ratio	0.28
Four-point bend strength	735 MPa

TABLE II Flexural strength test results

Void grade	Number of specimens	Average void diameter (μm)	Average void depth (μm)	Average nominal strength (MPa)
1	38	153 (19.1)[a]	231 (30.2)[a]	650 (42.6)[a]
2	47	241 (19.7)	287 (36.6)	615 (36.6)
3	47	312 (23.8)	319 (46.0)	572 (41.0)
4	37	470 (33.7)	390 (49.4)	523 (40.8)

[a] Standard deviation given in parentheses.

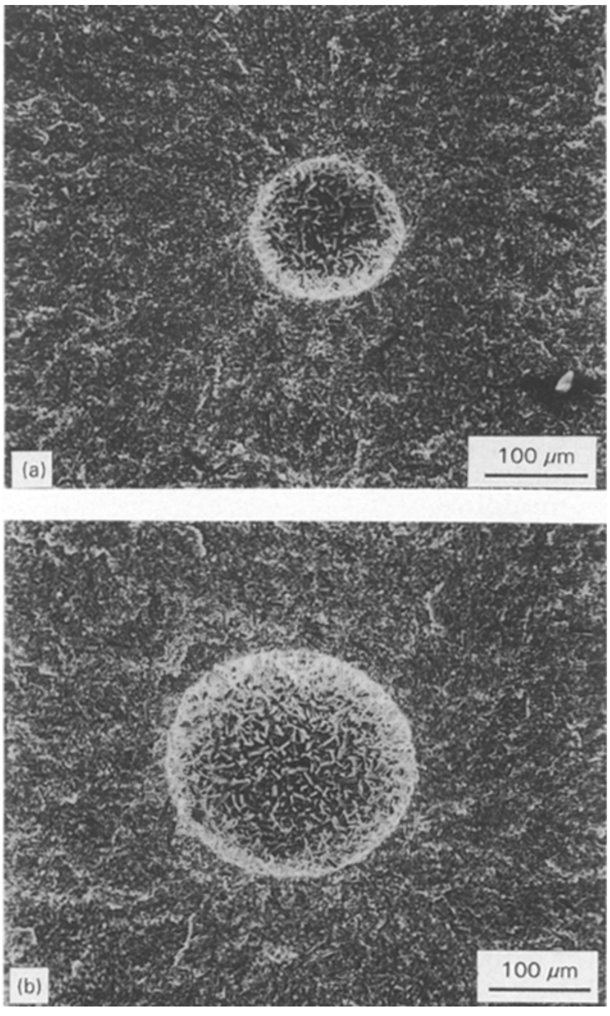

Figure 3 Artificially embedded voids. Average diameter: (a) 153 μm, (b) 241 μm, (c) 312 μm, (d) 470 μm.

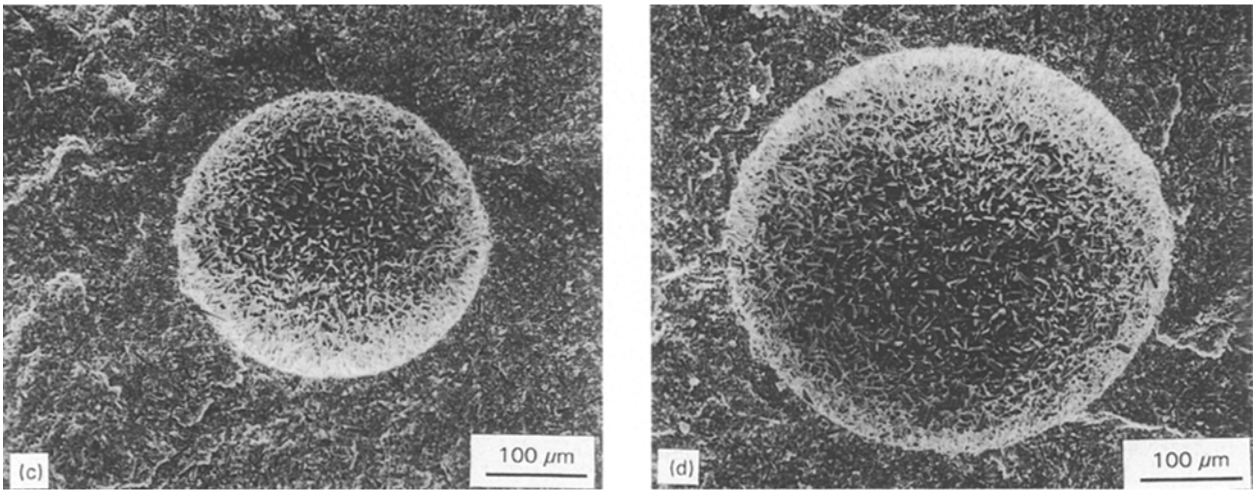

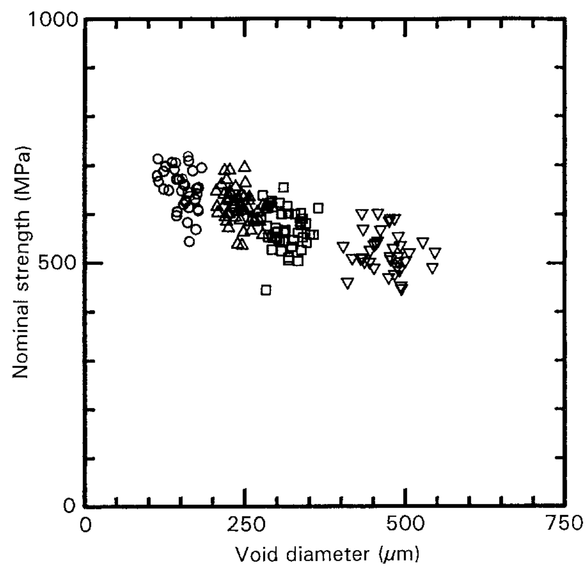

Figure 4 Nominal flexural strength versus void diameter. (○) 153 μm, (△) 241 μm, (□) 312 μm, (▽) 470 μm.

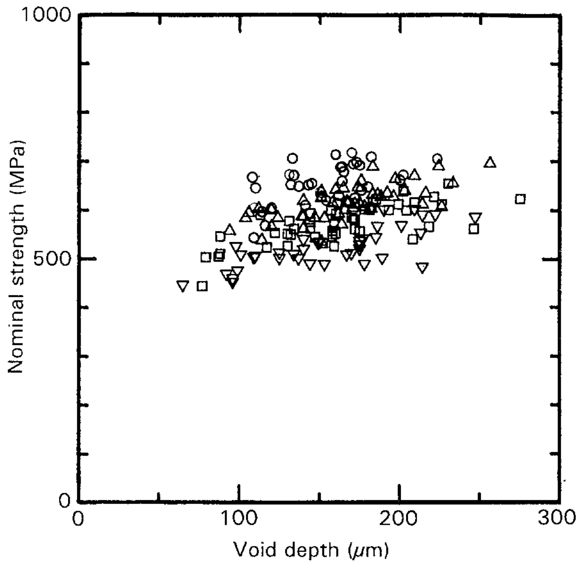

Figure 5 Nominal flexural strength versus void depth. For key, see Fig. 4

5. Comparison of experimental results and estimation from the fracture model

The estimated fracture loads from the Gibbs free energy versus the experimentally measured values are plotted in Fig. 6. The dashed line shows the averaged fracture load of the specimens with no artificial void. The intrinsic fracture load was approximately 900 N.

For the 470, 312, and 241 μm voids, good agreement can be observed between the estimated and experimental loads. For the 153 μm voids, however, the fracture loads were overestimated, compared with the experimental ones. The experimental fracture load is rather on the line of the intrinsic one.

The intrinsic fracture origins of this material are mainly voids of less than 100 μm according to a previous tensile test [19]. Specimens with voids of more than 241 μm were fractured from the artificially embedded voids. For specimens with 153 μm voids, 20% of the specimens fractured from origins other than the artificially embedded void (see Table II). This indi-

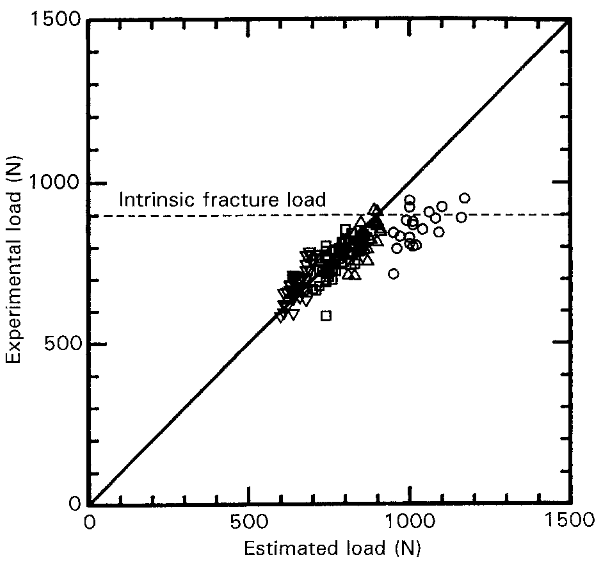

Figure 6 Experimental load versus estimated load. For key, see Fig. 4.

cates a transition of fracture origin occurring from the artificially embedded voids to the intrinsic flaws.

The transition may be explained by an interaction mechamism between the artifical flaw and the intrinsic flaws in ceramics. Some experimental work by Sakai and Miyajima [20] supports the existence of this kind of transition. It is also considered that interactions between intrinsic flaws play an important role in the fracture of ceramics.

6. Conclusion

The four-point flexural strengths of silicon nitrides containing a spherical void were measured. The data were compared with values estimated theoretically from an unstable energy criterion. The Gibbs free energy was micromechanically calculated using Eshelby's equivalent inclusion technique. Good agreement between the experimental and estimated values was obtained.

The discrepancy between the estimated and experimental loads for voids of small diameter indicates that interaction may occur between intrinsic flaws and an artificial void.

The present unstable energy criterion may provide a quantitive approach for further study of the fracture mechanism on brittle materials.

Acknowledgements

The authors thank Professors R.C. Bradt and M. Sakai for their valuable comments and E. Matsuo, H. Kino and K. Takita for their discussions. We also thank Y. Oishi and H. Miyata for their suggestions.

Appendix. Interaction energy calculation

Eshelby proposed replacing an inclusion by an ellipsoid which has elastic properties identical to those of the matrix and fictitious stress-free strains (eigenstrains) so that the same stress state of the inclusion is reproduced. The disturbed strain around the inclusion is then calculated by the following procedure [15].

First, we consider an ellipsoidal inclusion, Ω, in an infinite elastic body, D, as shown in Fig. A1. The functional form of the ellipsoid is expressed as

$$\frac{x_1^2}{a_1^2} + \frac{x_2^2}{a_2^2} + \frac{x_3^2}{a_3^2} \leqslant 1 \tag{A1}$$

The total strain, $u_{i,k}(x)$, generated by the inclusion, is expressed by

$$u_{i,k}(x) = -\int_{\Omega} C_{jlmn} G_{ji,lk}(x, x')\, e^*_{nm}(x')\,\mathrm{d}x' \tag{A2}$$

where $e^*_{nm}(x')$ is the eigenstrain. C_{jlmn} and $G_{ji,lk}(x, x')$ are the stiffness tensor of the matrix and the second derivative of Green's function. Green's function for an infinite and isotropic body is written as

$$G_{ji}(x - x') = \frac{\bar{x}_j\bar{x}_i/\bar{x}^3 + (3 - 4\nu)\delta_{ji}/\bar{x}}{16\pi(1 - \nu)\mu} \tag{A3}$$

where $\bar{x}_i = x_i - x_i'$ and $\bar{x} = (\bar{x}_i\bar{x}_i)^{1/2} \cdot \delta_{ji}$ is the Kronecker delta. μ and ν are the shear modulus and Poisson's ratio, respectively.

For a bending stress state, the eigenstrains are described by a function of a linear combination of the variables x_1, x_2 and x_3, and can be written as

$$e^*_{nm}(x) = e^p_{nm} y_p + e^{**}_{nm} \tag{A4}$$

where $y_p = x_p/a_p$. Then Equation A2 can be expressed as

$$u_{i,k}(y) = y_q S^{pq}_{ikmn} e^p_{nm} + S_{ikmn} e^{**}_{nm} \tag{A5a}$$

where

$$S^{pq}_{ikmn} = \frac{3}{4\pi} a_1 a_2 a_3 C_{jlmn} a_p a_q \int_S \frac{\xi_q\xi_p\xi_l\xi_k}{(a_1^2\xi_1^2 + a_2^2\xi_2^2 + a_3^2\xi_3^2)^{5/2}} \times [N_{ij}(\xi) D^{-1}(\xi)\,\mathrm{d}S(\xi)] \tag{A5b}$$

and

$$S_{ikmn} = \frac{1}{4\pi} a_1 a_2 a_3 C_{jlmn} \int_S \frac{\xi_l\xi_k}{(a_1^2\xi_1^2 + a_2^2\xi_2^2 + a_3^2\xi_3^2)^{3/2}} \times [N_{ij}(\xi) D^{-1}(\xi)\,\mathrm{d}S(\xi)] \tag{A5c}$$

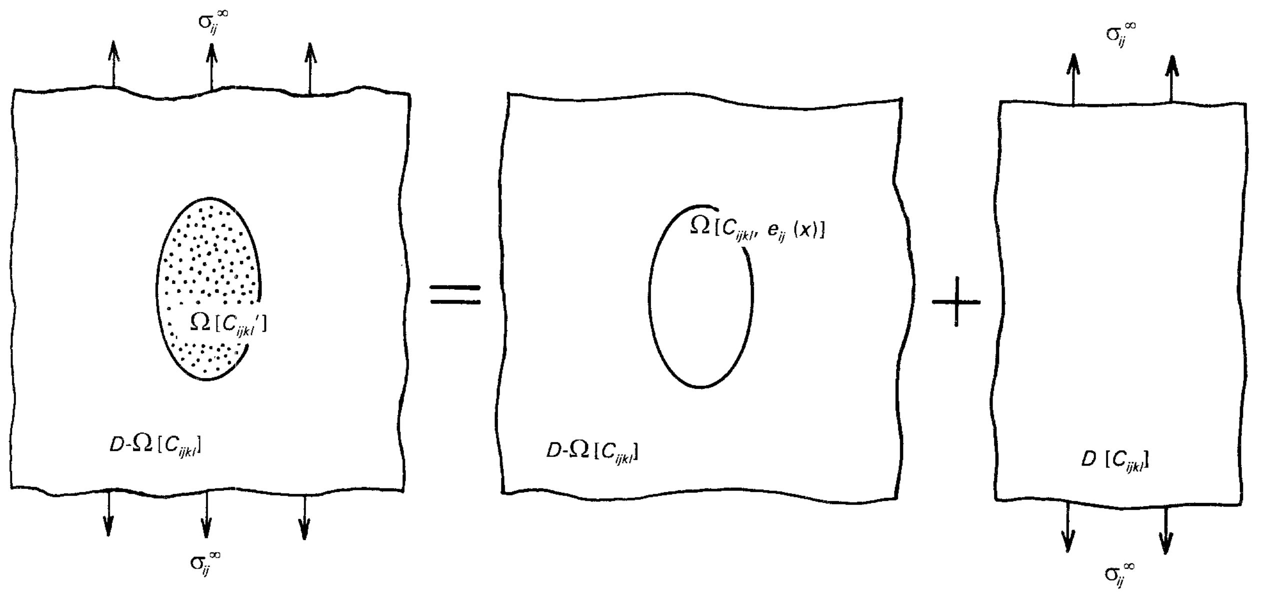

Figure A1 Eshelby's equivalent inclusion model.

where $\bar{\xi}_i$ is a unit vector and S represents the surface of the unit sphere. N_{ij} and D are the cofactor and the determinant of a matrix, K, respectively. The matrix elements of K are written as

$$K_{ik}(\bar{\xi}) = C_{ijkl}\bar{\xi}_j\bar{\xi}_l \tag{A6}$$

From Equation (A5a) and the relation of stress and strain, the stresses inside the replaced inclusion, which has elastic moduli identical to those of the matrix and the eigenstrains, are given by

$$\begin{aligned}\sigma_{st} = C_{stik}[&y_1(S^{p1}_{ikmn}e^p_{nm} - e^1_{ik} + E^1_{ik}) \\ &+ y_2(S^{p2}_{ikmn}e^p_{nm} - e^2_{ik} + E^2_{ik}) \\ &+ y_3(S^{p3}_{ikmn}e^p_{nm} - e^3_{ik} + E^3_{ik}) \\ &+ (S_{ikmn}e^{**}_{nm} - e^{**}_{ik} + E_{ik})]\end{aligned} \tag{A7}$$

where $y_q E^q_{ik} + E_{ik}$ is the strain in the presence of the applied stress. The stresses inside the inclusion, which has different elastic moduli from those of the matrix, are also given as

$$\begin{aligned}\sigma'_{st} = C^*_{stik}[&y_1(S^{p1}_{ikmn}e^p_{nm} + E^1_{ik}) \\ &+ y_2(S^{p2}_{ikmn}e^p_{nm} + E^2_{ik}) \\ &+ y_3(S^{p3}_{ikmn}e^p_{nm} + E^3_{ik}) \\ &+ (S_{ikmn}e^{**}_{nm} + E_{ik})]\end{aligned} \tag{A8}$$

where C^*_{stik} is the stiffness tensor of the inclusion.

Finally, 18 and 6 simultaneous equations

$$C_{stik}(S^{pq}_{ikmn}e^p_{nm} - e^p_{ik} + E^q_{ik}) = C^*_{stik}(S^{pq}_{ikmn}e^p_{nm} + E^q_{ik}) \tag{A9}$$

and

$$C_{stik}(S_{ikmn}e^{**}_{nm} - e^{**}_{ik} + E_{ik}) = C^*_{stik}(S_{ikmn}e_{nm} + E^{**}_{ik}) \tag{A10}$$

are obtained by requesting $\sigma_{st} = \sigma'_{st}$. In the present study, the right-hand side terms of Equations A9 and A10 are equal to zero, because $C^*_{stik} = 0$.

The unknown constants of the eigenstrains, e^p_{im} and e^{**}_{im} (Equation A4), are obtained by solving these 18 and 6 simultaneous equations. Once these eigenstrains have been determined, the interaction energy of Equation 4 can be obtained.

References

1. J. A. SALEM, S. R. CHOI, M. R. FREEDMAN and M. G. JENKINS, *J. Mater. Sci.* **27** (1992) 4421.
2. D. MUNZ, O. ROSENFELDER, F. GOEBBELS and H. REITER, in "Fracture Mechanics of Ceramics", Vol. 7, edited by R. C. Bradt, A. G. Evans, D. P. H. Hasselman, F. F. Lange and R. E. Tressler (Plenum Press, New York, 1986) p. 265.
3. A. OKADA and N. HIROSAKI, *Yogyo-Kyokai-Shi* (*J. Ceram. Soc. Jpn*) **95** (1987) 400.
4. J. HEINRICH and D. MUNZ, *Ceram. Bull.* **59** (1980) 1221.
5. *Idem, Commun. Am. Ceram. Soc.* **65** (1982) C34.
6. F. I. BARATTA, *J. Am. Ceram. Soc.* **61** (1978) 490.
7. *Idem, Commun. Am. Ceram. Soc.* **64** (1981) C3.
8. A. G. EVANS and G. TAPPIN, *Proc. Br. Ceram. Soc.* **20** (1972) 275.
9. A. G. EVANS, D. R. BISWAS and R. M. FULRATH, *J. Am. Ceram. Soc.* **62** (1979) 101.
10. D. J. GREEN, *ibid.* **63** (1980) 342.
11. G. G. TRANTINA and M. BARISHPOLSKY, *Eng. Fract. Mech.* **20** (1984) 1.
12. V. D. KRSTIC, *Acta Metall.* **33** (1985) 521.
13. J. D. ESHELBY, *Proc. R. Soc.* **A241** (1957) 376.
14. D. BROEK, "Elementary Engineering Fracture Mechanics", 4th Edn (Martinus Nijhoff, Dordrecht, 1986) p. 123.
15. T. MURA and T. MORI, "Maikuromekanikkusu (Micromechanics)" (Baifuukan, Tokyo, 1976) p. 23.
16. T. MURA, "Micromechanics of Defects in Solids" (Martinus Nijhoff, The Hague, 1982) p. 1.
17. M. TAYA and R. J. ARSENAULT, "Metal Matrix Composite" (Pergamon Press, Oxford, 1989) p. 82.
18. T. NOSE and T. FUJII, *J. Am. Ceram. Soc.* **71** (1988) 328.
19. A. KOKAJI, H. UCHIMURA and M. KAJI *J. Ceram. Soc. Jpn* **100** (1992) 1304.
20. M. SAKAI and T. MIYAJIMA, *J. Eur. Ceram. Soc.* **7** (1991) 249.

Received 26 May 1993
and accepted 5 May 1994